

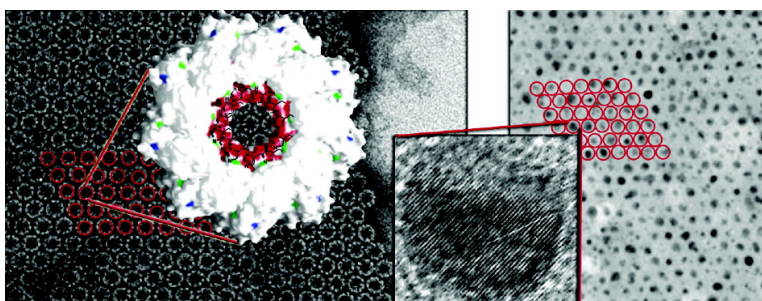
Communication

A Self-Assembling Protein Template for Constrained Synthesis and Patterning of Nanoparticle Arrays

R. Andrew McMillan, Jeanie Howard, Nestor J. Zaluzec, Hiromi K. Kagawa, Rakesh Mogul, Yi-Fen Li, Chad D. Paavola, and Jonathan D. Trent

J. Am. Chem. Soc., **2005**, 127 (9), 2800-2801 • DOI: 10.1021/ja043827s • Publication Date (Web): 09 February 2005

Downloaded from <http://pubs.acs.org> on March 24, 2009



More About This Article

Additional resources and features associated with this article are available within the HTML version:

- Supporting Information
- Links to the 15 articles that cite this article, as of the time of this article download
- Access to high resolution figures
- Links to articles and content related to this article
- Copyright permission to reproduce figures and/or text from this article

[View the Full Text HTML](#)

A Self-Assembling Protein Template for Constrained Synthesis and Patterning of Nanoparticle Arrays

R. Andrew McMillan,^{*,†} Jeanie Howard,[‡] Nestor J. Zaluzec,[§] Hiromi K. Kagawa,[‡] Rakesh Mogul,[‡] Yi-Fen Li,[‡] Chad D. Paaavola,[†] and Jonathan D. Trent[†]

NASA Ames Research Center, Moffett Field, California 94035, and
Argonne National Laboratory, Argonne, Illinois 60439

Received October 11, 2004; E-mail: amcmillan@5AMventures.com

We report here a general technique for patterning nanoparticle (NP) arrays using a genetically engineered crystalline protein template to direct constrained chemical synthesis. The heat-shock protein TF55 β spontaneously assembles into an octadecameric double-ring cage structure called a chaperonin,¹ which in turn readily assembles into two-dimensional (2D) crystalline arrays.² We genetically removed a loop on TF55 β that occludes the central pore of the assembled chaperonin and added a polyhistidine (His₁₀) sequence to its amino terminus. With these modifications, the solvent-accessible cores of assembled chaperonins possess 180 additional His residues, creating a region with enhanced affinity for metal ions that is spatially constrained by the interior dimensions of the chaperonin. When incubated with Pd(II), the chaperonin cores become sites for selectively initiating the chemical reduction of magnetic transition metal (TM) ions (either Ni²⁺ or Co²⁺) from precursor salts. This procedure yields arrays of bimetallic (here Ni–Pd or Co–Pd) nanoparticles with dimensions defined by the chaperonin. Furthermore, the NPs are patterned into arrays because the 2D crystalline template imparts longer-range order that extends across the engineered protein crystal. Target applications of these patterned NP arrays range from high-density data storage media to directing the catalytic growth of additional materials such as nanotubes on substrates.

We previously demonstrated that self-assembling chaperonins modified with simple point mutations could be used to organize metallic nanoparticles and semiconductor quantum dots.³ Here, we introduce an alternative strategy in which we engineer the structure of TF55 β to enhance the solvent accessibility of the chaperonin core and then functionalize it by attaching a peptide to the amino terminus of the subunit which is positioned inside the chaperonin. Two-dimensional crystals of these functionalized chaperonins promote chemical synthesis of alloyed NPs, while chaperonins without the His₁₀ modifications do not. The dimensions of the chaperonin cavities influence the geometry of the NPs, and the lattice structure of the 2D crystalline template imparts order, simultaneously patterning the NPs into arrays. We anticipate that this patterning technique can be extended to different classes of materials given the diversity of peptide sequences elucidated using screening techniques borrowed from biotechnology that are capable of interfacing with inorganic materials with a high degree of specificity.⁴

The chaperonin subunit protein TF55 β was originally cloned from a hyperthermophilic organism which thrives at 85 °C and pH 1–2. These robust proteins, even when mutated, tolerate a variety of modifications without losing their ability to self-assemble. This includes both the subunit self-assembly into chaperonins and the

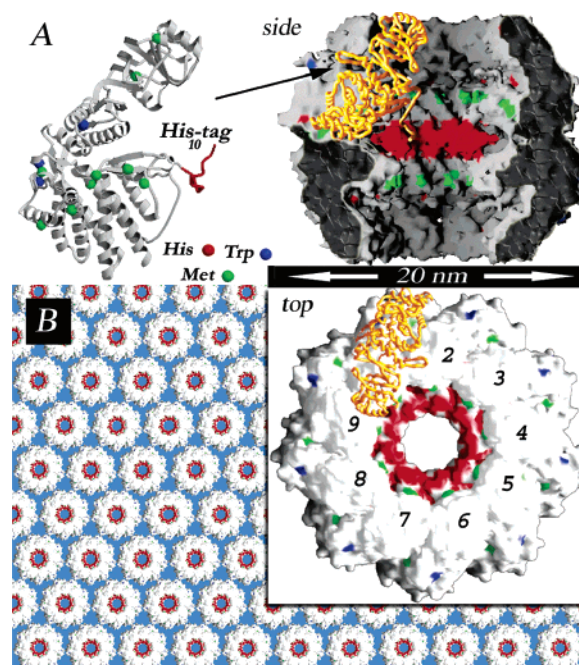


Figure 1. Assembly of engineered chaperonin templates. (A) Structures of the subunit (left) and the assembled chaperonin (right, cross section side- and top-views) highlight in red the accessible 10 nm diameter core functionalized with His. (B) Hexagonal packing of chaperonins into 2D crystals is the basis for patterning NP arrays.

chaperonin self-assembly into 2D crystals that we exploit as templates. We used structure-based protein design as a guide to functionalize the crystalline chaperonin template (Figure 1).

By deleting the apical loop amino acid residues and attaching the His₁₀ peptide to TF55 β , we increased both the solvent accessibility and the affinity for metal binding of the hollow cores of the chaperonin. When these modified subunits assemble into the chaperonin, they produce a 20 nm diameter cage structure with a core containing 180 additional imidazole groups from the 18 His₁₀ peptides. When further assembled into hexagonally packed 2D crystals, the cores of the His-containing chaperonins are uniformly distributed in a periodic lattice and serve as selective nucleation sites for constrained chemical synthesis and patterning of TM NPs.

We chose the 3d–4d binary TM alloy systems Ni–Pd and Co–Pd as target materials for several reasons. Protocols for solution synthesis by electroless deposition, where reduction of either Ni or Co by dimethylamine borane complex (DMAB) is initiated using Pd, have been reported.⁵ TM nanoparticles are routinely used in catalysis due to their well-known reactive properties. Bulk Ni–Pd alloys, which are ferromagnetic even at low concentrations of Ni, are promising candidates for use in magnetic data storage media.⁶ Thin films of Ni_xPd_{1-x} epitaxially grown on Cu substrates exhibit

* Current address: 5AM Ventures, 3000 Sand Hill Road, Menlo Park, CA 94025.

[†] Bioengineering Branch, NASA Ames Research Center.

[‡] SETI Institute, NASA cooperative agreement NCC2-1338.

[§] Materials Science Division, Argonne National Laboratory.

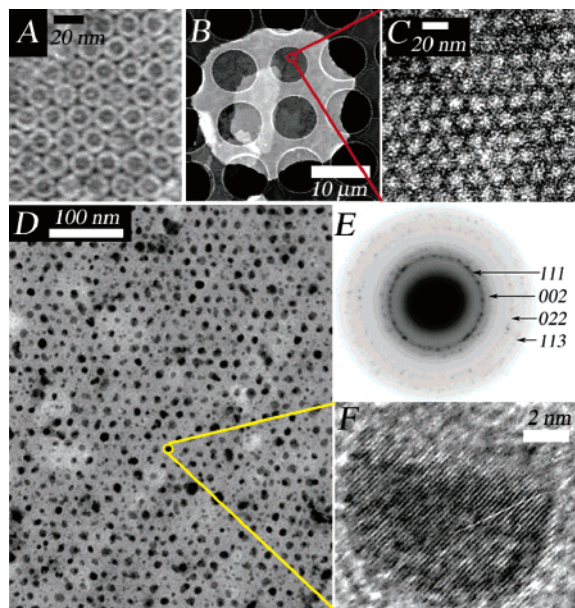


Figure 2. TEM imaging of a patterned array. (A) Uranyl acetate staining enables visualization of chaperonins in the 2D crystal templates. (B) Synthesis of Ni–Pd NPs enhances the contrast of the template in HAADF–STEM mode (unstained Ni–Pd array on Quantifoil, 200 kV). (C) Enlargement of a suspended region reveals a hexagonal array of clusters of small NPs. (D) Imaging at 60 kV (bright-field TEM) coalesces the clusters forming larger NPs 8–10 nm in diameter that retain the hexagonal arrangement. (E) SAED pattern of the array indexes to fcc. (F) HRTEM lattice imaging indicates that the coalesced Ni–Pd NPs are crystalline.

an *inverse* spin reorientation transition (*i*SRT) due to atomic size mismatch-induced lattice strain in these materials. Manipulation of this transition may be exploited in high-density nanoscale-patterned media.⁷ Finally, this synthetic strategy can also be applied to *3d–5d* ferromagnetic materials, such as CoPt, which exhibit high coercivity and magnetic anisotropy in the chemically ordered (fct) $L1_0$ phase.⁸

Reduction of Ni^{2+} or Co^{2+} by DMAB requires initiation by Pd^0 . To bind Pd to the His-rich regions within the template for electroless deposition, a preparation of 2D crystals was incubated with aqueous palladium(II) acetate and then dialyzed against a slightly acidic buffer (see Supporting Information for details). Palladium(II) is a soft metal ion and should tightly bind to the imidazole side chains of the histidines (N-donors) at neutral to basic pH, as well as to the few accessible tryptophans (N-donor) and methionines (S-donor) native to TF55 β .⁹ The dialysis step minimizes background from less tightly bound Pd species, such as $[\text{PdCl}_4]^{2-}$, which based on electrostatics, can associate with exposed Lys or Arg sidegroups that do not act as N-donors under these conditions.¹⁰ TEM analysis of unstained, Pd-enriched templates revealed a periodic distribution of alternating electron-dense regions reflecting the spacing of the protein crystal lattice. This suggests that Pd accumulates in the hexagonally packed His-rich chaperonin cores (see Supporting Information).

Synthesis of the Ni–Pd and Co–Pd arrays was performed on substrates suitable for quantitative HRTEM analysis (Figure 2). The Pd-enriched templates were applied to either micromachined carbon (Quantifoil) or etched SiN “window” substrates and then were perfused with a solution containing 1 g/L DMAB and either 1 mM NiSO_4 or 1 mM CoSO_4 to form the NPs.

Initial TEM characterization at 200 kV revealed the synthesis of small NPs (approximately 2 nm) that accumulate into hexagonally arranged clusters and uniformly decorate the template. The periodic distribution of these clusters across the protein crystal

suggests that NPs preferentially accumulate in the central regions of the hexagonally packed chaperonins (Figure 2C). Elemental maps using energy filtered (EF)-TEM of the C and Ni content of a Ni–Pd array confirm the hexagonal distribution of accumulated Ni and also suggest that the thin chaperonin templates possess monolayer regions (see Supporting Information).

While imaging arrays at low accelerating voltage (60 kV), we observed an interaction with the electron beam that coalesced each cluster of small NPs into larger NPs 8–10 nm in diameter (Figure 2D). This effect, which has been reported for palladium(II) acetate,¹¹ did not occur at 200 kV, but was reproduced by heating samples at 500 °C for 5 h in an inert environment. The arrays of larger coalesced NPs maintain the hexagonal distribution across the template representative of the periodic crystalline lattice; although, some distortion of longer-range order was observed due to deterioration of the thin organic template or to NP movement upon coalescence. Selected area electron diffraction (SAED) patterns confirm the larger annealed NP arrays index to (fcc), and X-ray analysis confirms bimetallic composition.

In conclusion, our template-directed approach to constrained nanomaterials synthesis is unique in that it enables simultaneous patterning of the NPs into arrays on substrates. The average size of the annealed NPs is representative of the interior dimensions of the modified chaperonins, and their arrangement in arrays reflects the 2D lattice of the template. Investigations into both the magnetic and catalytic properties of these bimetallic TM nanoarrays are underway.

Acknowledgment. We acknowledge financial support from the NASA Ames Center for Nanotechnology and from the Department of Energy under Contract BESMSW-31-109Eng38.

Supporting Information Available: Detailed procedures for synthesis and characterization of bimetallic NP arrays. This material is available free of charge via the Internet at <http://pubs.acs.org>.

References

- (1) Trent, J. D.; Nimmegern, E.; Wall, J. S.; Hartl, F. U.; Horwich, A. L. *Nature* **1991**, *354*, 490.
- (2) Koeck, P. J.; Kagawa, H. K.; Ellis, M. J.; Hebert, H.; Trent, J. D. *Biochim. Biophys. Acta* **1998**, *1429* (1), 40.
- (3) (a) McMillan, R. A.; Paavola, C. D.; Howard, J.; Chan, S. L.; Zaluzec, N. J.; Trent, J. D. *Nat. Mater.* **2002**, *1* (4), 247. (b) Mogul, R.; McMillan, R. A.; Paavola, C. D.; Trent, J. D.; Zaluzec, N. J. *Microsc. Microanal.* **2003**, *9* (Suppl 2), 274.
- (4) (a) Brown, S.; Sarikaya, M.; Johnson, E. *J. Mol. Biol.* **2000**, *299*, 725. (b) Naik, R. R.; Jones, S. E.; Murray, C. J.; McAuliffe, J. C.; Vaia, R. A.; Stone, M. O. *Adv. Funct. Mater.* **2004**, *14* (1), 25. (c) Whaley, S. R.; English, D. S.; Hu, E. L.; Barbara, P. F.; Belcher, A. M. *Nature* **2000**, *405*, 665.
- (5) (a) Brenner, A.; Riddell, G. E. *Proc. Am. Electroplating Soc.* **1947**, *34*, 156. (b) Kirsch, R.; Mertig, M.; Pompe, W.; Wahl, R.; Sadowski, G.; Bohm, K.-J.; Unger, E. *Thin Solid Films* **1997**, *305*, 248.
- (6) (a) Taylor, J. W.; Duffy, J. A.; Poulter, J.; Bebb, A. M.; Coper, M. J.; McCarthy, J. E.; Timms, D. N.; Staunton, J. B.; Itoh, F.; Sakurai, H.; Ahuja, B. L. *Phys. Rev. B* **2001**, *65*, 024442. (b) Seider, M.; Kaltofen, R.; Muschiol, U.; Lin, M.-T.; Schneider, C. M. *J. Appl. Phys.* **2000**, *87* (9), 5762.
- (7) (a) Muschiol, U.; Seider, M.; Schneider, C. M.; Lin, M.-T. *J. Appl. Phys.* **2001**, *89* (11), 6892. (b) Matthes, F.; Seider, M.; Schneider, C. M. *J. Appl. Phys.* **2002**, *91* (10), 8144.
- (8) (a) Sun, S.; Murray, C. B.; Weller, D.; Folks, L.; Moser, A. *Science* **2000**, *287*, 1989. (b) Baglin, J. E. E.; Folks, L.; Kellock, A. J.; Terris, B. D.; Weller, D. K. U.S. Patent 6,331,364, 2001.
- (9) (a) Appleton, T. G.; Pesch, F. J.; Wienken, M.; Menzer, S.; Lippert, B. *Inorg. Chem.* **1992**, *31*, 4410. (b) Dujardin, E.; Peet, C.; Stubbs, G.; Culver, J. N.; Mann, S. *Nano Lett.* **2003**, *3*, 413.
- (10) (a) Mertig, M.; Kirsch, R.; Pompe, W. *Appl. Phys. A* **1998**, *66*, S723. (b) Behrens, S.; Rahn, K.; Habicht, W.; Bohm, K.-J.; Rosner, H.; Dinjus, E. *Adv. Mater.* **2002**, *14*, 1621.
- (11) (a) Dieluwit, S.; Pum, D.; Sleytr, U. B. *Supramol. Sci.* **1998**, *5*, 15. (b) Stark, T. J.; Mayer, T. M.; Griffis, D. P.; Russell, P. E. *J. Vac. Sci. Technol.* **1991**, *9* (6), 3475.

JA043827S